Poultry Science®

Integrative transcriptomics and proteomics analysis provide a deep insight into goose astrovirus-host interactions during GAstV infection

Jianzhou Shi ,[*,†,1] Qianyue Jin,[‡,1] Jinbing Zhao,[*] Jinran Yu,[*] Xianyi Yu,[*] Guirong Sun,[†,§] and Lunguang Yao[*,‖,¶,2]

[*]*School of Life Science, Nanyang Normal University, Nanyang, Henan 473061, China;* [†]*The Shennong Laboratory, Zhengzhou, Henan 450046, China;* [‡]*Key Laboratory of Animal Immunology, Henan Academy of Agricultural Sciences, Zhengzhou, Henan, China;* [§]*Animal Science and Technology, Henan Agricultural University, Zhengzhou, Henan 450046, China;* [‖]*Henan Field Observation and Research Station of Headwork Wetland Ecosystem of the Central Route of South-to-North Water Diversion Project, Nanyang, Henan 473061, China; and* [¶]*Henan Provincial Engineering and Technology Center of Health Products for Livestock and Poultry, Nanyang, Henan 473061, China*

ABSTRACT Goose astrovirus (**GAstV**) is a newly discovered astrovirus. GAstV causes gout and death in 4- to -16-day-old goslings. For the past few years, fatal gout, the cardinal clinical symptom of gosling infected with GAstV, has been spreading rapidly in some goose Chinese farms, which caused continuous economic losses to the goose breeding industry in China. Currently, several underlying mechanisms involved in viral replication, inflammatory reaction, virions release, and viral pathogenesis of GAstV remain to be elucidated. In this study, we explored the mechanisms of GAstV-host interactions, the transcriptome and proteome profiles of GAstV-infected LMH cells were sequenced by RNA-seq and data-independent acquisition (**DIA**) techniques, respectively, and followed using an integrative analysis. Compared with uninfected LMH cells, a total of 322 differentially expressed genes (**DEG**) (195 up-regulated, 127 down-regulated) and 36 differentially expressed proteins (**DEP**) (31 up-regulated, 5 down-regulated) were detected. Nine DEGs were randomly selected for further validation by quantitative real-time polymerase chain reaction (**qPCR**). Through GO and KEGG enrichment analysis, DEG and DEP were significantly enriched in several important cellular signaling pathways, including MAPK, PI3K-Akt, cAMP, chemokine, calcium, phospholipase D, Ras, TNF, IL-17, Rap1, NF-kappa B signaling pathways, indicating that GAstV affects cell growth and immune signaling. This study provided an overview of changes in transcriptome and proteome profiles of GAstV-infected LMH cells, therefore, providing a crucial basis to further explore the mechanisms of GAstV-host interactions.

Key words: goose astrovirus, transcriptome, proteome

2024 Poultry Science 103:104287
https://doi.org/10.1016/j.psj.2024.104287

INTRODUCTION

Astroviruses cause enteritis in humans and a variety of animals. Astroviruses first were identified in the fecal samples of children with gastroenteritis in 1975 (Madeley and Cosgrove, 1975). Astroviruses are small, nonenveloped, positive-sense, single-stranded RNA viruses belonging to the family Astroviridae (Wang et al., 2021a). The astrovirus genome (approximately 6.0−7.7 kb in length) contains a 5′-untranslated region (UTR), a 3′-UTR, 3′ open reading frames (**ORF**), and a poly (A) tail. The genome is organized into 3 to 4 open ORFs (ORF1a, ORF1b, and ORF2). ORF1a and ORF1b encode the viral nonstructural proteins, and ORF2 encodes a viral structural protein (capsid) (Diakoudi et al., 2023). Astroviruses have the potential to cross species barriers and adapt to new host species (Roach and Langlois 2021). The host range of astroviruses is wide, with diarrhea or intestinal disease as the main symptoms (Liu et al., 2023). Astroviruses often cause coinfections with many other enteric viruses, for instance, adenoviruses and noroviruses (Neves et al., 2021). Astrovirus infections pose a major problem for the poultry industry, causing many adverse effects, such as decreased egg production, breeding disorders, poor weight gain, and even significantly increased mortality (Sajewicz-Krukowska et al., 2021). Goose astrovirus (**GAstV**) is a newly identified viral pathogen

Received June 11, 2024.
Accepted August 28, 2024.

[1]These authors contribute equally.

[2]Corresponding author: lunguangyao@163.com

threatening waterfowl. Epidemiological studies have found that there are 2 (type 1 and type 2) circulating genotypes of GAstV in China (Cen et al., 2023; Li et al., 2021; Zhang et al., 2022). Goslings are more susceptible to GAstV, and severe visceral gout, joint gout, hemorrhage, and swelling of the kidneys are the main symptoms, exhibiting a high prevalence throughout China (Xu et al., 2024). After the first GAstV infection was identified in 2016 (Zhang et al., 2017), growing evidence is revealing a rapid spread of GAstV across various regions in China causing serious losses to the goose-breeding industry (Li et al., 2023). However, the mechanisms by which GAstV makes use of host cells to complete viral replication, virion release, viral pathogenesis, and immuno-inflammatory responses are still unclear. As an emerging virus, research on GAstV is still in the primary stage and many questions remain unknown.

Both transcriptomics and proteomics can reflect the gene expression of organisms in a certain growth and development stage or under certain physiological conditions, and they are powerful tools for studying physiological and biochemical states. Transcriptomics is a useful and widely applied molecular sequencing technique. Proteomics is an essential technique to determine the existence, protein type, and morphology of proteins in organisms, including protein expression level, translation and modification, and protein interaction (Wu et al., 2021). Because of the higher accuracy of multi-omics data compared to single-omics analysis, it is widely used to disclose the full picture of biological systems (Ritchie et al., 2015; Xing et al., 2023). The combined analysis of transcriptomics and proteomics is a practical method to study the internal regulatory mechanisms of organisms. In recent years, differential transcriptome and proteome combined data before and after viral infection have enabled a comprehensive explanation of the host of viral infection to identify potential biomarkers that play vital roles in virus-host interactions (Greco and Cristea 2017; Yang et al., 2018).

The purpose of the present study was to combine transcriptomic and proteomic methods to measure the difference of host cell leghorn male hepatocellular (**LMH**) data before and after GAstV infection, and to analyze the expression changes of host genes and proteins before and after GAstV infection. To ascertain potential biomarkers that play crucial roles in virus-host interactions.

MATERIALS AND METHODS

Viruses and Cells

GAstV (GAstV XX strain, belonging to goose astrovirus type 1, GenBank number: MN337323) and leghorn male hepatocellular (LMH) cell were friendly provided by Henan Provincial Key Laboratory of Animal Immunology, Henan Academy of Agricultural Sciences (Zhengzhou, China).

Sample Collection and Testing

GAstV (GAstV XX strain) was propagated on LMH cells. After the virus was inoculated, LMH cells were cultured in Dulbecco's modified Eagle's medium (**DMEM**) (Solarbio, Beijing, China), supplemented with penicillin-streptomycin and 10% fetal bovine serum (FBS, Gibco, Waltham) for 48 h post infection (p.i.), at 37°C in the presence of 5% CO_2. At the same time, uninfected LMH cells were set as control. There were 3 replicates in the infection group (TA1, TA2, TA3) and the control group (TB1, TB2, TB3).

Medium from 6 cell culture bottles were discarded, washed with sterile phosphate-buffered saline (PBS, pH 7.4) buffer, digested with trypsin, centrifuged at 1,000 rpm for 10 min, and cells were collected. The cells were washed 3 times with PBS buffer and centrifuged at 1000 rpm for 10 min. The cells were stored in freeze-storage tubes, frozen in liquid nitrogen.

The 6 samples were detected respectively to determine whether LMH cells in the infected group were infected by GAstV, and whether LMH cells in the control group were not infected by GAstV. Two methods of PCR and droplet digital PCR (ddPCR) were used for detection. The specific primers used in the common PCR identification method were designed according to the ORF1b sequence of the AstV/SDPY/Goose/1116/17 strain (GenBank number: MH052598.1).

We designed a primer pair specific for GAstV (F: 5′-ACCCCTGGTTATCCAAAATTTAAGT-3′ and R: 5′-CCGCCAGAAGAGAGGCTTGGGCAAC-3′) based on the ORF1b sequence of RNA polymerase gene of AstV/SDPY/Goose/1116 /17 strain (GenBank number: MH052598.1). The expected fragment size is 420 bp. Total viral RNA was extracted from 6 cell samples, and the virus cDNA was reverse-transcribed to be used as PCR template. The final volume of each PCR assay was 50 μL, comprising 22 μL double-distilled H_2O (**ddH_2O**), 1 μL of the primer pair (10 mM each), 1 μL template DNA, and 25 μL 2×EasyTaq PCR SuperMix (TransGen Biotech Co., Ltd., Beijing, China). The cycling conditions were as follows: initial denaturation at 94°C for 5 min; 30 cycles of 94°C for 30 s, 58°C for 30 s, and 72°C for 1 min; and final extension at 72°C for 10 min. ddH_2O was used as a negative control. The PCR products were identified by 1.5% agarose gel electrophoresis. The detection method was the ddPCR method established in our laboratory (Shi et al., 2024). The specific primers and probes were designed and synthesized based on the ORF2 gene of AstV/SDPY/Goose/1116/17 strain (GenBank number: MH052598.1). The sequence of PCR upstream primer was 5′-GCCCAGATAGACAGCAGGAT-3′. The sequence of PCR downstream primer was 5′-GCGAGGGAGTAGCCTGTATT-3′. The sequence of probe was 5′-FAM-ACCTGCCTCTGCCAGTGGCACC-BHQ1-3′. The LMH cells of 6 samples were extracted, RNA concentration quantification and viral nucleic acid reverse transcription were performed. The 6 samples were tested using the established ddPCR assay. The viral copy

number of GAstV and clinical samples were quantified by the TD-1 Droplet Digital PCR System (TargetingOne, Beijing, China) according to the product's instruction manual. In brief, the 30 μL ddPCR system mixture and 180 μL oil were then loaded into the designated location of the droplet generation chip, and small droplets were generated on the droplet manufacturing machine. PCR amplification was performed on a T100 thermal cycling apparatus. After PCR amplification, a droplet chip reader was used to read the data of each small droplet unit that has been PCR individually, which was analyzed with droplet reader software. The ddPCR assay was repeated 3 times.

Transcriptome Examination and Analysis

Transcriptome sequencing was performed using eukaryotic reference transcriptome assay techniques. The experimental procedure of strand-specific library construction was as follows. Total RNA was extracted from LMH cells by Trizol reagent kit (Invitrogen, Carlsbad, CA) as stated by the manufacturer's operation instructions. RNA quality was evaluated and checked. After total RNA was extracted, rRNAs were removed to keep mRNAs and ncRNAs, that is, mRNA was purified. The mRNAs and ncRNAs were fragmented into small fragments by means of fragmentation buffer and reverse transcribed into cDNA using random primers. Second-strand cDNA were produced using DNA polymerase I, RNase H, dNTP (dUTP in place of dTTP) and buffer. Next, the cDNA was purified, end repaired, poly (A) added, and ligated to Illumina sequencing adapters. Then, Uracil-N-Glycosylase was applied to digest the second-strand cDNA. Finally, the digested produces were size selected using agarose gel electrophoresis, PCR amplified, and sequenced with Illumina HiSeq^{TM} 2500 by Guangzhou Gene Denovo Biotechnology Company (China). In a word, the experimental flow included total RNA extraction, RNA quality detection, rRNA removal, RNA fragmentation (200−500 nt), first strand cDNA synthesis, UNG treatment, PCR amplification, and sequencing. The differences in gene expression levels were examined. The conditions for screening differentially expressed genes (**DEG**) were the expression difference multiple $|\log_2\text{fold change}|>1$, and false discovery rate (**FDR**) <0.05.

The DEGs were categorized by functional enrichment, and the significantly enriched functional classifications and signal pathways were found. Gene ontology (**GO**) is a worldwide standardized gene functional classification system which has 3 ontologies: molecular function (**MF**), cell component (**CC**), and biological process (**BP**). GO offers a dynamically updated orderly vocabulary and strictly defined concepts to define the properties of genes and their products in organisms. The GO enrichment analysis provides all the GO terms that is significantly enriched in DEGs compared to the genome context and filtered out the DEGs corresponding to the biological functions. First, all DEGs are mapped to GO terms in the GO database, the number of genes for each term is calculated, and the GO terms that are significantly enriched in DEGs compared to the genomic context are defined with hypergeometric tests. The calculated *P*-value is corrected by FDR, with FDR <0.05 as the threshold. A GO term that meets this condition is defined as one that is significantly enriched in DEGs. The analysis can identify the leading biological functions performed by DEGs. Genes often interact and play a role in certain biological functions.

Pathway-based study contributes to further comprehend the biological function of genes. Kyoto Encyclopedia of Genes and Genomes (**KEGG**) is the main common pathway database. Pathway enrichment study shows that metabolic or signal transduction pathways are significantly enriched in DEGs compared to the genome-wide context. Pathway Enrichment Analysis Genes generally play a certain biological function through interaction. The calculated *p*-value is carried out FDR correction, with FDR <0.05 as the threshold. The pathways that satisfy the conditions are defined as those that are significantly enriched in DEGs. That is, the DEGs were correlated with pathways according to the KEGG database to identify the differences between the GAstV-infection group (TA) and the control group (TB) at the level of pathway.

Proteome Examination and Analysis

Proteome sequencing was implemented using data-independent acquisition (DIA) quantitative proteomics technique. The main steps included protein extraction, denaturation, reductive alkylation, enzymatic hydrolysis, and peptide desalting, and the establishment of a database, data collection, protein qualitative and quantitative analysis. DIA combined the advantages and characteristics of traditional proteomics "shotgun" and mass spectrometry absolute quantitative "gold standard" selective reaction monitoring/multiple reaction monitoring (**SRM/MRM**) techniques. The whole scanning range of the mass spectrum was divided into several Windows, and all ions in each window were selected, broken and detected at high speed and cycle, to obtain all the fragment information of all ions in the sample. Compared with the traditional data-dependent acquisition mode (DDA), it has the advantages of panoramic scanning, high data utilization, high repeatability, high quantitative accuracy, and data backtracking. Therefore, DIA technology could obtain more accurate and rich results, which was suitable for protein detection of large sample sizes and complex systems. The difference analysis of proteins was based on the quantitative results of proteins to screen out the proteins with significant changes in abundance between groups. First, the Student's T-test with R was used to obtain the *P*-value. In order to reduce the false positive rate, the multiple hypothesis test was performed to correct the *P*-value, and the method Benjamini and Hochberg (**BH**) was applied to obtain the FDR value. According to the

screening threshold of differently expressed proteins, the absolute value of Fold change (**FC**) was greater than 1.5 times ($|\log_2 1.5| \approx 0.58$), and the Q value obtained by correcting the P value was <0.05. Proteins with significant differences between groups were screened. Differences in protein to GO each term mapping database (http://www.geneontology.org/), and calculation of the difference of each term protein, and had a GO function protein list differences of protein number statistics. Hypergeometric tests were then applied to identify GO entries that were significantly enriched in differential proteins compared to the background. In vivo, different differential proteins coordinated their biological functions. Pathway-based analysis was helpful to further understand the biological functions of differential proteins. KEGG was the main public database on the Pathway.

Pathway significant enrichment analysis was conducted using KEGG Pathway as unit and hypergeometric test was applied to find out the Pathway of significant enrichment in different proteins compared with the whole background. Through significant enrichment of Pathway, the most important biochemical metabolic pathways and signal transduction pathways involved in differential proteins can be identified.

Combined Analysis of Transcriptome and Proteome

Firstly, we obtained the quantitative analysis results of proteome and transcriptome, extracted the corresponding proteins and transcripts. Then the differential protein and the corresponding differential transcription relationship pairs were extracted to show the consistency of the relationship pairs. Finally, proteins and associated transcripts are localized to relevant metabolic pathways.

Quantitative Real-Time PCR Analysis

Each viral nucleic acid RNA sample was reverse transcribed using the HiScript III All-in-one RT SuperMix reagent kit (Vazyme, Nanjing, China), following the product's instructions. The cDNA was immediately amplified or stored at -80°C for later use. To confirm alterations in mRNA expression levels, we conducted a quantitative real-time polymerase chain reaction (**qPCR**). RT-PCR was performed with a QuantStudio 1 Plus System Fluorescent quantitative PCR instrument (Thermo Fisher). In this study, the primers for qPCR were designed by Primer Premier 5.0 software. The 20 μL final reaction system consisted of 10 μL of 2 × SG Fast qPCR Master Mix, 0.4 μL (10 μM) of each of the reverse and forward primers each, 7.2 μL of RNase-free ddH_2O, and 2 μL of template. QPCR amplification was performed at 95°C for 3 min (initial steps), 45 cycles of 95°C for 15 s and 60°C for 30 s. After the qPCR, a standard curve was drawn, and the actual viral RNA copies were calculated based on the curve. The $2^{-\Delta\Delta Ct}$ method was employed for evaluating mRNA expression levels, with normalization to glyceraldehyde-3-phosphate dehydrogenase (**GAPDH**). Relative mRNA expression levels were calculated by the $2^{-\Delta\Delta Ct}$ method with GAPDH mRNA as an endogenous control. The specific primer sequences were detailed in Table 1.

Table 1. Sequence of primers.

Primer	Sequence (5′−3′)	Length (bp)	Tm (°C)
GAPDH-F2	GAACATCATCCCAGCGTCC	190	58
GAPDH-R2	ATCAGCAGCAGCCTTCACTAC		57.2
HELZ2-F2	TGGTGACCTTCAGTTCGCA	192	57.6
HELZ2-R2	CGTTGGAGTGAGCCTTGGT		58
IFI6-F1	GACCAGAACGTCCACAAAGC	130	57.7
IFI6-R1	GAGTAGCAGTAGTCCCTCCAGAA		57.4
ORF1-F1	CAAGGGAAGGGTTGAGAAGC	216	58.8
ORF1-R1	AGGATTACAAAGGGCAGCGT		59.0
AOC1-F4	ATGGAAGGAGGAAAAGGGC	104	58.1
AOC1-R4	GGTTGTTCTGGTTGTAGAGGCT		57.8
OASL-F1	CCACATCCTCGCCATCATC	190	58.8
OASL-R1	CCCCAGTGCGTCGTAAGC		59.5
ZNFX1-F1	CCCAAACATCTATGAAACCCG	177	59.6
ZNFX1-R1	GGACTGCCTCCGTGACCA		59.2
FETUB-F2	CTCAGCAAACAGTTGTGGAAGA	203	58.0
FETUB-R2	GGCTCAGTTGGACAGTCATCA		58.0
RBP4A-F1	ATCCTGAGGGGCTGTTTCTAC	119	57.6
RBP4A-R1	ACAGACATCCCAGTTATTGAAGAGT		58.4
ELOVL2-F2	AGAAATACCTCACTCAGGCACAG	226	58.0
ELOVL2-R2	TTCTTGACTTCTGTTGTGACGG		57.8

RESULTS

Testing of Samples

Using PCR and the established ddPCR detection method of the GAstV in our laboratory (Shi et al., 2024), 6 samples were identified, respectively. The results showed that TA1, TA2, and TA3 in the infected group were infected by viruses, while TB1, TB2, and TB3 in the control group were not infected by viruses (Figures 1 and 2).

The Number of Significantly Differentially Expressed Genes and Proteins

As shown in Figures 3A−3C, compared with the control group TB, 322 genes with significant differences were screened from the infected group TA, of which 195 genes were up-regulated and 127 genes were down-regulated. GAstV-infected LMH cells significantly changed the expression levels of 36 proteins in LMH cells, with 31 significantly different proteins were up-regulated and 5 significantly different proteins were down-regulated in Figures 3D−3F. The up-regulated proteins included HELZ2 (helicase with zinc finger 2), IFI6 (interferon alpha inducible protein 6), KRT40 (keratin 40), ORF2 (capsid protein), RPL23A (ribosomal protein L23a), TMSB15B (thymosin beta 15B), ORM1 (orosomucoid 1), PSPH (phosphoserine phosphatase), PFKFB3 (6-phosphofructo-2-kinase/fructose-2,6-biphosphatase 3), MARCKS (myristoylated alanine rich protein kinase C

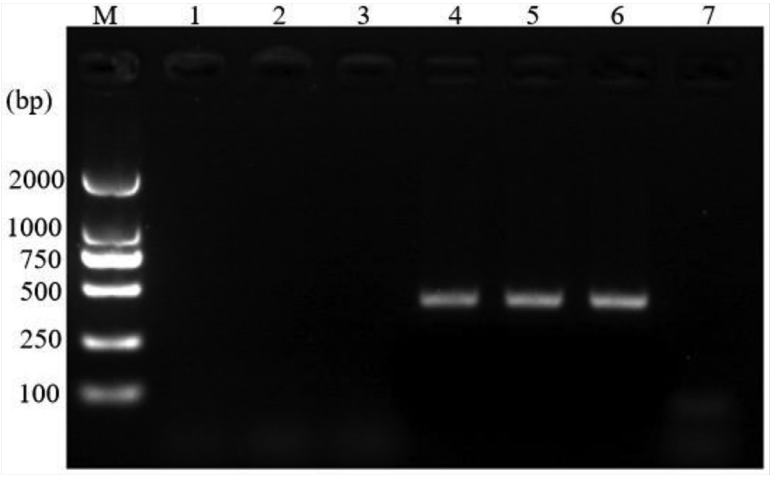

Figure 1. Six samples were detected by the GAstV PCR assay. M: DNA Marker. Lanes 1-7: TB1, TB2, TB3, TA1, TA2, TA3, and NC, respectively. TB: the control group; TA: the infection group. NC: ddH_2O was the negative control of the template.

substrate), PIT54 (PIT54 protein), A2ML1 (alpha-2-macroglobulin-like 4), MARCKSL1 (MARCKS like 1), OASL (2′−5′-oligoadenylate synthetase like), NUF2 (kinetochore complex component), CCDC125 (coiled-coil domain-containing protein 125), NEGR1 (neuronal growth regulator 1), ALCAM (activated leukocyte cell adhesion molecule), CSRP1 (cysteine and glycine rich protein 1), ADGRG2 (adhesion G protein-coupled receptor G2), IFIT5 (interferon induced protein with tetratricopeptide repeats 5), CLIC3 (chloride intracellular channel 3), PRDM2 (PR/SET domain 2), MAPK1IP1L (mitogen-activated protein kinase 1 interacting protein 1-like), MPZL1 (myelin protein zero like 1), PLIN2 (perilipin 2), IFITM5 (dispanin subfamily A member 2b-like), ORC4 (origin recognition complex subunit 4), ZNFX1 (zinc finger NFX1-type containing 1), LRRFIP1 (LRR binding FLII interacting protein 1), ACTG1 (actin, cytoplasmic 2-like). The down-regulated proteins included FETUB (fetuin B), RBP4A (retinol binding protein 4 A, plasma), CLCC1 (chloride channel CLIC like 1), Nat8 (N-acetyltransferase 8), TMEM14C (transmembrane protein 14C-like).

GO Analysis for the Transcriptome and Proteome Combined Analysis

In Figure 4A, the original 4-quadrant figure was upgraded, and the upgraded 9-quadrant figure further refined the changes of genes and proteins. The graph was divided into 9 quadrants by the dotted lines of the horizontal and vertical coordinates. The dashed line on the horizontal axis indicated the difference factor threshold of the transcriptome. The dashed line on the vertical axis indicated the difference factor threshold of the proteome. The genes/proteins outside the threshold line

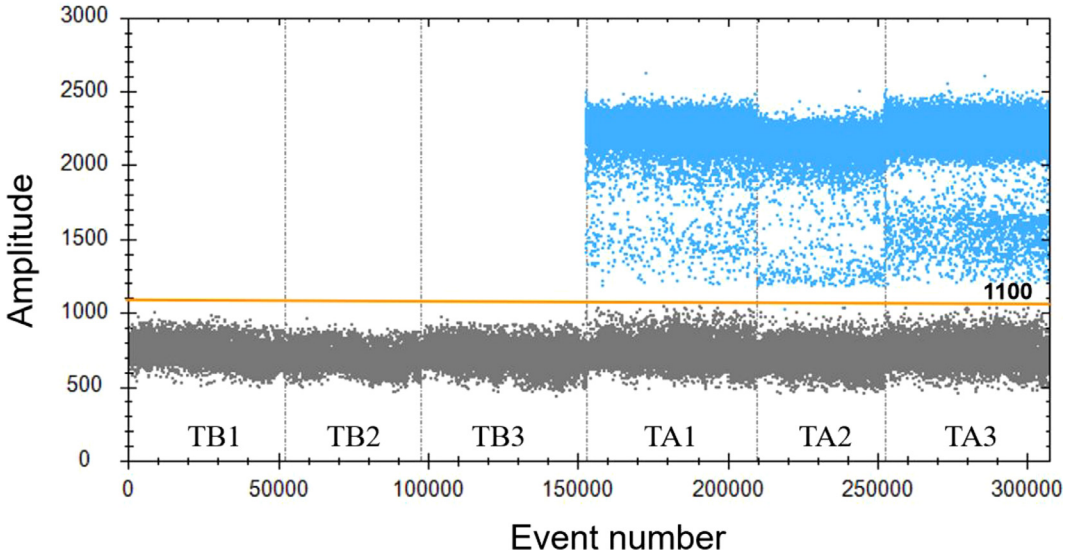

Figure 2. Six samples were detected by the GAstV ddPCR assay (Shi et al., 2024). Lanes 1-6 (divided by vertical black dotted lines): the fluorescence amplitude of TB1, TB2, TB3, TA1, TA2, and TA3, respectively. Blue dots indicated positive droplets. Gray dots indicated negative droplets. The orange horizontal line indicated the partition threshold.

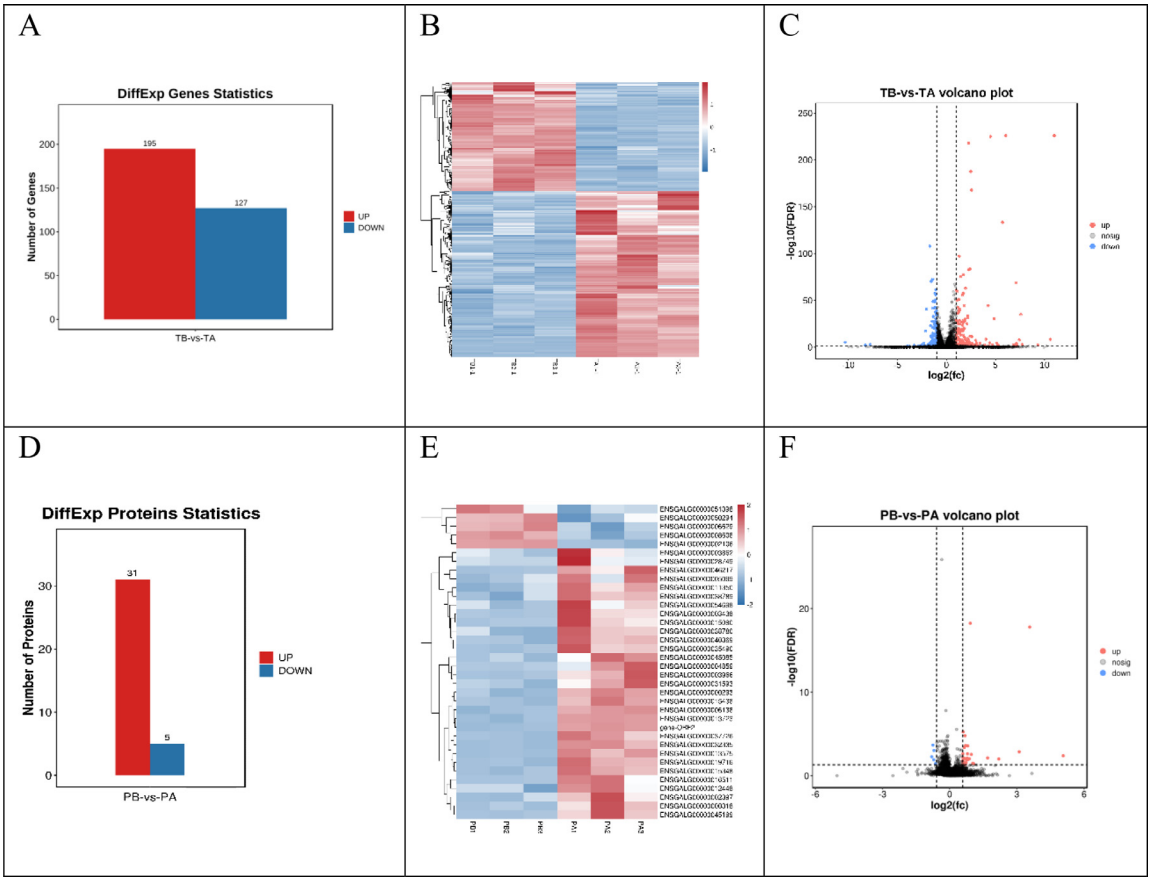

Figure 3. The significantly differentially expressed genes and proteins in the GAstV -infection group (TA) and the control group (TB). In Figure C and F, the 2 vertical dashed lines are the thresholds for the expression of multiple of difference, the horizontal dashed line represents the threshold of significance level. (A) The number of significantly differentially expressed genes. (B) Cluster heat map of differentially expressed genes. (C) Volcano map of differentially expressed genes. (D) The number of significantly differentially expressed proteins. (E) Cluster heat map of differentially expressed proteins. (F) Volcano map of differentially expressed proteins.

indicated significant differences, and the genes/proteins inside the threshold line indicated nonsignificant differences. The horizontal coordinate was the protein difference multiple (log2). The vertical coordinate was the transcriptome difference multiple (log2). The top of the figure was the correlation coefficient and *P*-value of the transcriptome and proteome association. Each dot represented a gene/protein. Black dots indicated nondifferentiated proteins and genes. Red dots indicated the same or opposite trend of gene and protein change. Green dots indicated differential expression of genes but nondifferential expression of proteins. Blue dots indicated that genes were not differentially expressed, but proteins were differentially expressed. If the difference multiple was reached and the *P*-value was not reached, it was shown as a gray dot. In quadrants 3 and 7, mRNA and corresponding protein differential expression patterns were consistent.

In Figure 4B, Venn figure compared all mRNAs and proteins in the group, and also compared the number of different mRNAs and proteins. Transcriptome represented the genes detected, and proteomics represented the proteins detected. All genes indicated the genes detected. All proteins indicated the detected proteins. Differential genes meant the different genes. Differential proteins meant the different proteins. In Figures 4C, 4D, and 4E, GO term histogram of gene number showed the number of differentially expressed mRNAs (red), proteins (green), and co-associated genes (blue) annotated on the GO term. In Figure 4F, the histogram of gene number of Pathway showed the number of differentially expressed mRNAs (red), proteins (green) and co-associated genes (blue) annotated on Pathway.

As shown in Figure 4A, in the third quadrant, there are 17 significant DEGs (red). They are HELZ2 (helicase with zinc finger 2), IFI6 (interferon alpha inducible protein 6), KRT40 (keratin 40), CLIC3 (chloride intracellular channel 3), PFKFB3 (6-phosphofructo-2-kinase/fructose-2,6-biphosphatase 3), MARCKS (myristoylated alanine rich protein kinase C substrate), MT4 (metallothionein 4), PIT54 (PIT54 protein), OASL (2′−5′-oligoadenylate synthetase like), CSRP1 (cysteine and glycine rich protein 1), IFIT5 (interferon induced protein with tetratricopeptide repeats 5), PSPH (phosphoserine phosphatase), ZNFX1 (zinc finger NFX1-type containing 1), MARCKSL1 (MARCKS like 1), NAB2 (NGFI-A binding protein 2), ORF1 (nonstructural polyprotein), ORF2 (capsid protein). In the 7th quadrant, there are 4 significant DEGs (red). They are FETUB (fetuin B), RBP4A (retinol binding protein 4 A, plasma), ELOVL2 (ELOVL fatty acid elongase 2), AOC1 (amine oxidase, copper containing 1).

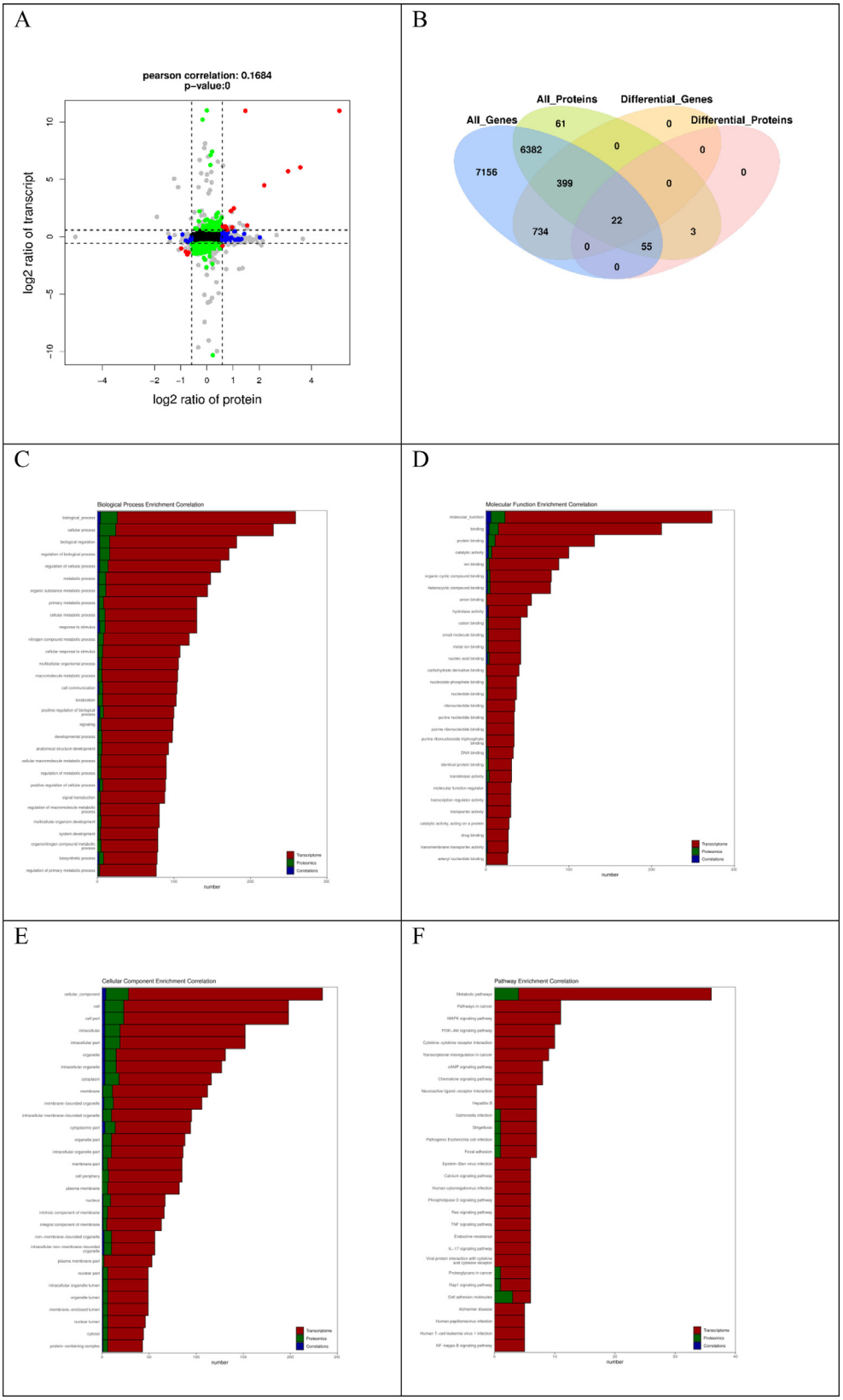

Figure 4. GO and KEGG analysis results for the transcriptome and proteome combined analysis. Red: Transcriptome. Green: Proteomics. Blue: Correlations. (A) Nine-quadrant (considering *P*-values) of TB-vs-TA. (B) Venn of TB-vs-TA. (C) Histogram of biological process (BP) Enrichment Correlation of TB-vs-TA in GO database. Red: Transcriptome. Green: Proteomics. Blue: Correlations. (D) Histogram of molecular function (MF) Enrichment Correlation of TB-vs-TA in GO database. Red: Transcriptome. Green: Proteomics. Blue: Correlations. (E) Histogram of cellular component (CC) Enrichment Correlation of TB-vs-TA in GO database. Red: Transcriptome. Green: Proteomics. Blue: Correlations. (F) Histogram of number of genes in Pathway enrichment results for the transcriptome and proteome combined analysis. Red: Transcriptome. Green: Proteomics. Blue: Correlations.

In the GO analysis of the correlation between transcriptome and proteome, biological process (**BP**) enrichment correlation of TB-vs-TA (Figure 4C), the following terms were included, cellular process, biological regulation, regulation of biological process, regulation of cellular process, metabolic process, organic substance metabolic process, primary metabolic process, cellular metabolic process, response to stimulus nitrogen compound metabolic process, cellular response to stimulus, multicellular organismal process, macromolecule metabolic process, cell communication, localization, positive regulation of biological process, signaling, developmental process, anatomical structure development, cellular macromolecule metabolic process regulation of metabolic process, positive regulation of cellular process, signal transduction, regulation of macromolecule metabolic process, multicellular organism development, system development, organonitrogen compound metabolic process, biosynthetic process, regulation of primary metabolic process.

Molecular function (**MF**) enrichment correlation of TB-vs-TA (Figure 4D), the following terms were included, binding, protein binding, catalytic activity, ion binding, organic cyclic compound binding, heterocyclic compound binding, anion binding, hydrolase activity, cation binding, small molecule binding, metal ion binding, nucleic acid binding, carbohydrate derivative binding, nucleoside phosphate binding, nucleotide binding, ribonucleotide binding, purine nucleotide binding, purine ribonucleotide binding, purine ribonucleotide triphosphate binding, DNA binding, identical protein binding, transferase activity, molecular function regulator, transcription regulator activity, transporter activity, catalytic activity, acting on a protein, drug binding, transmembrane transporter activity, adenyl nucleotide binding.

Cellular component (**CC**) enrichment correlation of TB-vs-TA (Figure 4E), the following terms were included, cell, cell part, intracellular, intracellular part, organelle, intracellular organelle, cytoplasm, membrane, intracellular membrane-bounded organelle, organelle lumen, membrane-bounded organelle, cytoplasmic part, organelle part, intracellular organelle part, membrane part, cell periphery, plasma membrane, nucleus, intrinsic component of membrane, integral component of membrane, nonmembrane-bounded organelle, intracellular nonmembrane-bounded organelle, plasma membrane part, nuclear part, intracellular organelle lumen, membrane-enclosed lumen, nuclear lumen, cytosol, protein-containing complex.

In the pathway analysis of the correlation between transcriptome and proteomics, metabolic pathways enrichment correlation of TB-vs-TA (Figure 4F), the following terms were included, pathways in cancer, MAPK signaling pathway, PI3K-Akt signaling pathway, cytokine-cytokine receptor interaction, transcriptional misregulation in cancer, cAMP signaling pathway, chemokine signaling pathway, neuroactive ligand-receptor interaction, hepatitis B, Salmonella infection, Shigellosis, pathogenic Escherichia coli infection, focal adhesion, Epstein-Barr virus infection, calcium signaling pathway, human cytomegalovirus infection, phospholipase D signaling pathway, Ras signaling pathway, TNF signaling pathway, endocrine resistance, IL-17 signaling pathway, viral protein interaction with cytokine and cytokine receptor, proteoglycans in cancer, Rap1 signaling pathway, cell adhesion molecules, Alzheimer disease, Human papillomavirus infection, human T-cell leukemia virus 1 infection, NF-kappa B signaling pathway.

Network Analysis Reveals Key Proteins and Key Gene Associations

As shown in Figure 5, up-regulated key genes included SLC7A3, ZNFX1, IL18, OASL, IFIT5, UNC13B, IFI6, ORF1, KRT40, PIT54, HELZ2, EPHA2, ORF2, HSD11B2, CLIC3, PFKFB3, CEBPB, and CSRP1. Down-regulated key genes included RBP4A, FETUB, ELOVL2, ENOX1, AOC1, and SPIA1. Up-regulated key proteins included HELZ2, OASL, MT4, MARCKS, SLC7A3, ORF2, IFI6, EEF1A2, MARCKSL1, and KRT40. Down-regulated key proteins included RBP4A and EETUB.

Quantitative Real-Time PCR Verification

The expression of some (AOC1, IFI6, HELZ2, ORF1, ZNFX1, FETUB, RBP4A, ELOVL2, and OASL) key DEGs were verified by qPCR. Among the DEGs, 9 genes were randomly selected for qPCR verification, specifically AOC1, IFI6, HELZ2, ORF1, ZNFX1, FETUB, RBP4A, ELOVL2, and OASL (Figure 6). The qPCR validation used the bar chart, corresponding to the Y-axis, and GAPDH was used for each sample as an endogenous control. The expression changes reported by qPCR were consistent with those detected by RNA-seq, indicating that the RNA-seq data was accurate.

DISCUSSION

Since 2017, the new GAstV was an emerging pathogenic virus that has resulted in huge economic losses to China's goose breeding industry. The host range of astroviruses is wide, and the main symptoms are diarrhea or intestinal disease (Jakubczak et al., 2021; Opriessnig et al., 2020; Wang et al., 2021b). GAstV is spread among poultry and poses a high risk to the poultry industry.

Transcriptomics and proteomics are both effective tools for studying gene expression. Gene expression is regulated by a lot of factors, and a single omics method frequently cannot fully explain biological phenomena. The description of biological events at the gene level is not exactly the same as the description at the protein level. The transcriptome is the intermediate state of gene expression at the transcriptional level, and merely reflects the potential protein expression, and the protein is the expression of the actual function. Thus,

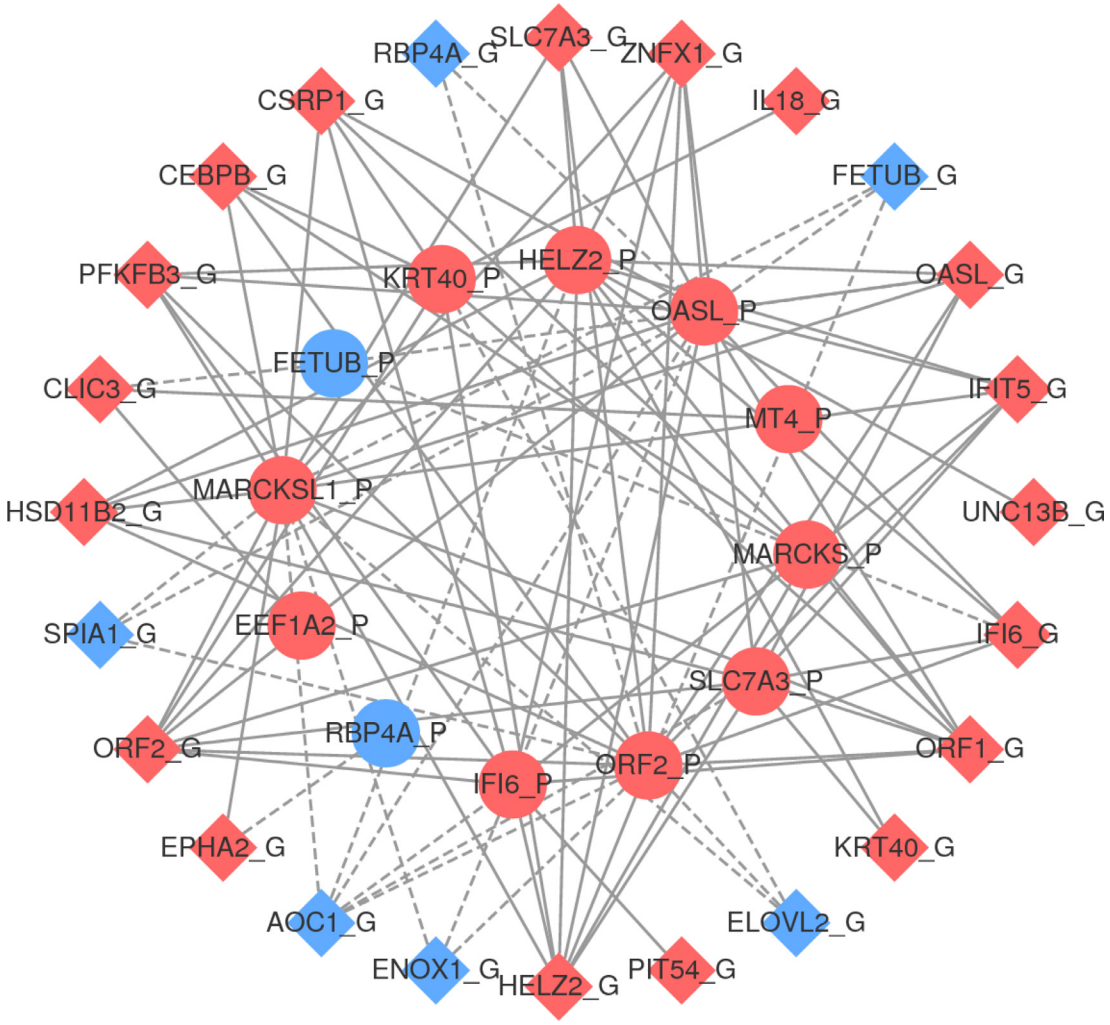

Figure 5. Network map of key proteins and key genes. Round: Protein. Square: Gene. Red: Up-regulated. Blue: Down-regulated. Solid line: Positive correlation. Dashed line: Negative correlation.

proteomics is essential for the study of the biological function. Combining transcriptomic data and proteomic data can efficiently study the physiological and biochemical states of organisms, in an attempt to grasp the regulation of genes as a whole (Miao et al., 2023; Wang et al., 2019a; Wu et al., 2021). Consequently, using the advantages of transcriptomics and proteomics, we can not only obtain a complete map of the physiological changes of organisms, but also clarify the regulatory mechanisms of organisms from different levels (Chen et al., 2021; Lu et al., 2022).

In this study, transcriptional changes and protein changes in host LMH cells infected with viruses were comprehensively analyzed. The study aimed to analyze data on differences between virus-infected and virus-uninfected host cells by transcriptome and proteome to detect potential biomarkers that play a vital role in virus-host interactions.

Many genes presented significantly changed expression levels in the GAstV-infected LMH cells. Significantly, the up-regulated DEGs (ZNFX1, OASL, IFIT5, IFI6, HELZ2, ORF1, ORF2) and DEP were predominantly associated with metabolic pathways, AMPK signaling pathway, HIF-1 signaling pathway, fructose and mannose metabolism, carbon metabolism, biosynthesis of amino acids, glycine, serine and threonine metabolism, nucleocytoplasmic transport, transcriptional misregulation in cancer, TNF signaling pathway, IL-17 signaling pathway, synaptic vesicle cycle. PI3K-Akt signaling pathway, MAPK signaling pathway, Ras signaling pathway, Rap1 signaling pathway, NOD-like receptor signaling pathway, cytosolic DNA-sensing pathway, cytokine-cytokine receptor interaction, steroid hormone biosynthesis, aldosterone-regulated sodium reabsorption, viral protein interaction with cytokine and cytokine receptor, thus, indicating that GAstV could affect cell growth and cellular immune signaling. Both ORF1 (nonstructural polyprotein) and ORF2 (capsid protein) are viral proteins that are highly expressed in host cells. IFI6 (interferon alpha inducible protein 6, IFN-α-inducible protein 6) is a hydrophobic protein with antiviral activity containing a signal peptide that is localized in the ER (Dukhovny et al., 2019; Richardson et al., 2018). IFI6 can delay cell apoptosis (Cheriyath et al., 2007; Sajewicz-Krukowska et al., 2021). IFI6 has no effect on entry and early viral translation, but it does delay RNA replication and reduce late translation of viral genes. IFI6 inhibits different flaviviruses and contributes to the antiviral effect of IFN-I against these viruses (Berthoux 2020).

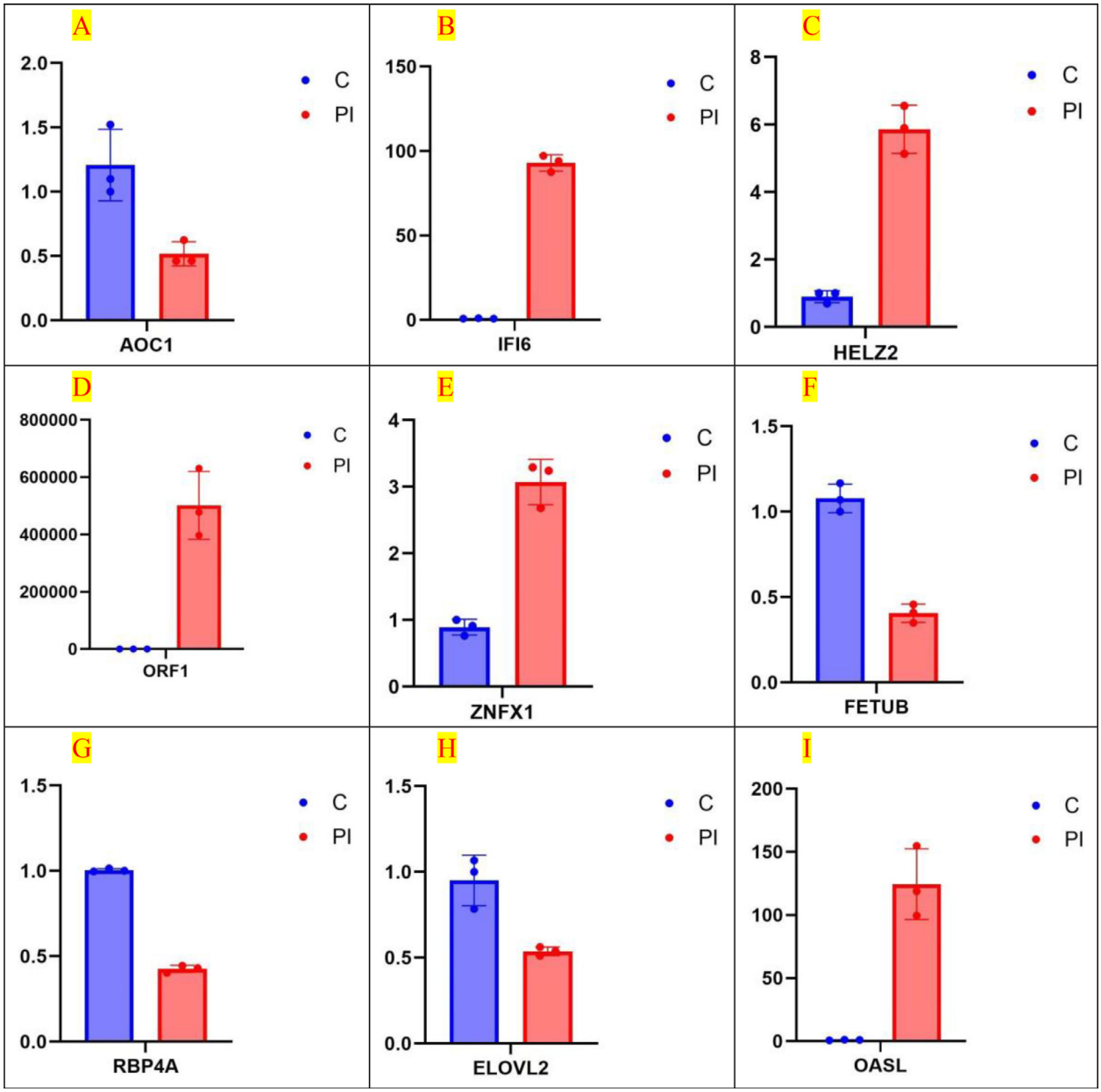

Figure 6. The expression of 9 key DEGs were verified by qPCR. Blue is the control group (TB), uninfected LMH cells. Red is the infection group (TA), infected LMH cells, post infection (p.i., PI). Y-axis: relative expression.

Interferon-induced proteins with tetratricopeptide repeats (**IFIT**) are sequentially degraded helix-turn-helix motifs responsible for protein-protein interactions (Abbas et al., 2013). 4 family members have been confirmed. Most mammals encode all family members, and IFIT5 is the only family member found in birds (Zhang et al., 2019). IFIT5 is an antiviral response gene that is active against RNA viruses, for example, avian influenza virus, Newcastle disease virus and duck Tembusu virus (Rong et al., 2018; Sajewicz-Krukowska et al., 2021; Wu et al., 2020). IFIT5 has antiviral activity. IFIT5 is involved in viral replication, translation initiation, cell migration, cell proliferation, and signaling regulation. IFIT5 is an important modulator of the human signaling pathway RIG-I/IFIT5/MAVS (Zhang et al., 2013). And, IFIT5 specifically antagonizes RNA viruses by sequestering viral nucleic acids in chickens (Li et al., 2020; Santhakumar et al., 2018). ISGs family of oligoadenylate synthetases (**OAS**), capable of synthesizing 2′ to 5′ oligoadenylate, induce RNA degradation by means of activating a latent RNase (RNase L) (Kristiansen et al., 2011). Oligoadenylate synthetase-like (**OASL**), is associated with OAS proteins through its N-terminal OAS-like domain, but has characteristic changes at the active site, and therefore lacks 2′ to 5′oligoadenylate synthetase activity. OASL is a vital and possibly RIG-I-dependent inhibitor of RNA virus replication that prevents the virus from escaping from innate immunity. GAstV-GD induces high levels of expression of OASL. An important host factor that restricts viral replication in LMH cells (Sajewicz-Krukowska et al., 2021; Zhu et al., 2015). CAstV (chicken astrovirus) is also effective in increasing OASL mRNA levels in vivo. OASL has antiviral activity and is directly and rapidly induced by way of viral infection by interferon regulatory factor (**IRF**)-3 and IFN signaling

(Marques et al., 2008; Schoggins et al., 2011). RIG-I expression activates IFN, which leads to toxicity, while OASL expression does not activate IFN induction, unlike RIG-I expression. Even in the presence of viral inhibition, OASL can enhance innate host defense and thus enhance immunity (Zhu et al., 2015). Zinc finger NFX1-type containing 1 (**ZNFX1**), a superfamily 1 helicase, has been recognized as a new dsRNA sensor capable of enhancing antiviral responses (Wang et al., 2019b). ZNFX1 is an interferon-stimulating protein associated with the mitochondrial outer membrane that binds to dsRNAs and interacts with MAVS proteins to promote the type I IFN response early in viral infection (Blasi et al., 2022). ZNFX1 has antiviral capabilities. ZNFX1 was upregulated in early bovine endometrial response induced by interferon tau (Forde et al., 2012), and spleen tissues of the chicken infected with dsRNA analogues (Kim and Zhou, 2015). Helicase with zinc finger 2 (HELZ2) is a transcription factor belonging to the nucleoprotein family. Expression of HELZ2 is induced by interferon treatment and plays an important role in RNA processing, gene expression regulation, development, and viral infection (Huntzinger et al., 2023). HELZ2 is a key transcriptional regulator in lipid metabolism (Li et al., 2016). Meanwhile, down-regulated DEGs (RBP4A, FETUB, ELOVL2, AOC1) and DEPs were primarily involved in metabolic pathways, fatty acid metabolism, biosynthesis of unsaturated fatty acids, fatty acid elongation, arginine and proline metabolism, tryptophan metabolism, histidine metabolism, chemical carcinogenesis-DNA adducts, cysteine and methionine metabolism, selenocompound metabolism, indicating that GAstV could interfere with the host metabolism. Amine oxidase copper-containing 1 (**AOC1**) is a secreted glycoprotein that catalyzes the degradation of putrescine and histamine. Polyamines and their diamine precursor putrescine, which exist widely in organisms, play a key role in cell growth and cell proliferation. Although AOC1 plays an important role in the regulation of polyamine decomposition, the molecular mechanism of its expression is unclear. It has been reported that the expression of AOC1 was downregulated due to the inactivation of WT1 (Wilms Tumor Protein, WT1), which was presumed to break the balance of pro-growth and pro-differentiation signals, thus favoring a proliferative phenotype (Kirschner et al., 2014).

DNA methylation of the elongation of very long chain fatty acids-like 2 (**ELOVL2**, ELOVL fatty acid elongase 2) promoter is one of the most robust molecular biomarkers for chronological age. ELOVL2 encodes a transmembrane protein that is involved in the synthesis of very long polyunsaturated fatty acids (**PUFA**). ELOVL2 is an enzyme that elongates long chain omega-3 andomega-6 (LC) PUFAs, precursors of 22: 6n-3, docosahexaenoic acid (**DHA**) and very long chain (**VLC**) PUFAs, all playing vital roles in retina biology. ELOVL2 plays an essential role in retinal biology and photoreceptor renewal, a key process associated with age-related eye diseases, for example, age-related macular degeneration (**AMD**) (Chao and Skowronska-Krawczyk 2020). Fetuin B (**FETUB**) is a cysteine proteinase inhibitor that exhibits potentially destructive activity of their target cysteine proteases, with many conserved N-glycosylation sites, species-specific O-glycosylation sites and 2 cystatin (**CY**) domains. FETUB may play a regulatory role in a variety of biological processes, such as acute inflammatory responses, female infertility, fish organogenesis, and tumor suppression. FETUB was originally recognized in rats in acute inflammation. FETUB is involved in mucosal immunity. As the first barrier against pathogen infection, the innate immune system plays a vital role in all organisms. FETUB plays an important role in innate immunity (Li et al., 2017). Human plasma retinol-binding protein (**RBP4**) is a fatty acid-binding protein (Perduca et al., 2018). RBP4A (retinol binding protein-4 A, plasma) is the only known carrier of vitamin A in plasma (Montenegro et al., 2022). RBP4 is a serum biomarker in the diagnosis and prognosis of hepatocellular carcinoma (Wan et al., 2024). Adipokines, including RBP4, play a crucial role in the pathogenesis of psoriasis (Gaoet al., 2023). In this study, DEGs were in 252 pathway enrichment, and 138 candidate genes with pathway annotations were included. The expression levels of key genes in metabolism-related pathways were down-regulated, including ELOVL2 (fatty acid metabolism); PCK1 (citrate cycle); PCK1, ALDOB, FBP2 (glycolysis/gluconeogenesis); ALDOB, FBP2, HAO2 (carbon metabolism). The expression of key genes related to immune processes was up-regulated, including IL8L1, IL8, IFIH1 (RIG-I-like receptor signaling pathway); IL8L1, IL8, TNFAIP3 (NOD-like receptor signaling pathway); and MAP3K8, IL8L1, IL8 (Toll-like receptor signaling pathway). Two recent studies, one of which analyzed changes in host genes in the kidneys of goslings infected with GAstV through a comprehensive analysis of global transcriptome and metabolic network pathways (Liu et al., 2023). Another study identified DEGs in primary goose kidney tubular epithelial cells after GAstV-2 infection by RNA sequencing analysis (Guo et al., 2024). The results showed that most of the key genes in the metabolic pathways of fatty acid metabolism, citrate cycle (TCA cycle), glycolysis/gluconeogenesis, and carbon metabolism were inhibited in the kidneys of goslings with gout symptoms and in primary goose kidney tubular epithelial cells infected with GAstV-2, both in vivo and in vitro. Whereas, in the immune pathways, such as the RIG-I like receptor signaling pathway, the NOD-like receptor signaling pathway, and the Toll-like receptor signaling pathway, where most of the key genes in the immune processes were up-regulated. These results are consistent with our findings that GAstV infection causes up-regulation of immune responses and down-regulation of metabolism.

The cellular innate immune system plays a key role in mounting the initial resistance to virus infection. GAstV infection of host LMH cells mainly affected cell cycle and immune signaling. Integrating transcriptomic and proteomic data, there were differences in the expression of

multiple genes and proteins between infected and uninfected hosts, ORF1, ORF2, ZNFX1, OASL, IFIT5, IFI6, HELZ2, RBP4A, FETUB, ELOVL2, and AOC1. To identify potential biomarkers that play a key role in GAstV interaction with its host. It is expected to be a candidate diagnostic marker for LMH cells infected with GAstV and may provide a new target for the diagnosis and treatment of GAstV in the future. Nevertheless, the potential mechanisms of GAstV-host interactions required further experimental validation.

CONCLUSIONS

Through GO and KEGG enrichment analysis, there were differences in the expression of multiple genes and proteins between infected and uninfected hosts, ORF1, ORF2, ZNFX1, OASL, IFIT5, IFI6, HELZ2, RBP4A, FETUB, ELOVL2, and AOC1. DEGs and DEPs were significantly enriched in several important cellular signaling pathways, including MAPK, PI3K-Akt, cAMP, chemokine, calcium, phospholipase D, Ras, TNF, IL-17, Rap1, NF-kappa B signaling pathways, indicating that GAstV affects cell growth and immune signaling.

ACKNOWLEDGMENTS

Funding: The present work was supported by the Key Research Project of the Shennong Laboratory (SN01-2022-05); Research and Practice Project on Research based Teaching Reform in Undergraduate Universities in Henan Province (2022SYJXLX079); Nanyang Normal University Science and Engineering STP project (2024STP006); Nanyang Normal University laboratory open project (SYKF2023066); the Nanyang Science and Technology Research Project (KJGG136 and RKX009); College students practice teaching activity innovation project of Nanyang Normal University (SPCP2024273 and SPCP2024300); Science and technology Innovation Leading Talent Project of the central plains of China (244200510040) and Henan Field Observation and Research Station of Headwork Wetland Ecosystem of The Central Route of South-to-North Water Diversion Project. Thanks for the sequencing platform and/or bioinformation analysis of Gene Denovo Biotechnology Co., Ltd (Guangzhou, China).

Ethics statement: All the experimental protocols were approved by the Animal Care and Use Committee of Nanyang Normal University (2024NYNU019) prior to the initiation of the study. The related animal experiments were conducted according to the rules and requirements of the Animal Care & Use Committee of Nanyang Normal University, China.

Author contributions: Jianzhou Shi: Conceptualization, Writing-original draft, Data curation, and Validation. Qianyue Jin: sample collection and Validation. Jinbing Zhao: Writing-review and editing. Jinran Yu: animal feeding and sample collection. Xianyi Yu: animal feeding and sample collection. Guirong Sun: Supervision, Funding acquisition. Lunguang Yao: Validation, Supervision, Funding acquisition, and Project administration. All authors read and approved the final manuscript.

DISCLOSURES

The authors declare that they have no known competing financial interests or personal relationships that could have appeared to influence the work reported in this paper.

REFERENCES

Abbas, Y. M., A. Pichlmair, M. W. Górna, G. Superti-Furga, and B. Nagar. 2013. Structural basis for viral 5'-PPP-RNA recognition by human IFIT proteins. Nature 494:60–64.

Berthoux, L. 2020. The restrictome of flaviviruses. Virol. Sin 35:363–377.

Blasi, G., E. Bortoletto, M. Gasparotto, F. Filippini, C.-M. Bai, U. Rosani, and P. Venier. 2022. A glimpse on metazoan ZNFX1 helicases, ancient players of antiviral innate immunity. Fish Shellfish Immunol 121:456–466.

Cen, X., G. Chen, and H. Zhang. 2023. Research Note: Isolation and complete genome analysis of a genotype II goose astrovirus in Sichuan Province, China. Poult Sci. 102:102800.

Chao, D. L., and D. Skowronska-Krawczyk. 2020. ELOVL2: Not just a biomarker of aging. Transl. Med. Aging 4:78–80.

Chen, S., Y. Li, Y. Zhao, G. Li, W. Zhang, Y. Wu, and L. Huang. 2021. iTRAQ and RNA-Seq analyses revealed the effects of grafting on fruit development and ripening of oriental melon (Cucumis melo L. var. makuwa). Gene 766:145142.

Cheriyath, V., K. B. Glaser, J. F. Waring, R. Baz, M. A. Hussein, and E. C. Borden. 2007. G1P3, an IFN-induced survival factor, antagonizes TRAIL-induced apoptosis in human myeloma cells. J. Clin. Invest 117:3107–3117.

Diakoudi, G., A. Buonavoglia, F. Pellegrini, P. Capozza, V. I. Vasinioti, R. Cardone, C. Catella, M. Camero, A. Parisi, L. Capozzi, J. A. Mendoza-Roldan, D. Otranto, K. Bànyai, V. Martella, and G. Lanave. 2023. Identification of new astroviruses in synanthropic squamates. Res. Vet. Sci 161:103–109.

Dukhovny, A., K. Lamkiewicz, Q. Chen, M. Fricke, N. Jabrane-Ferrat, M. Marz, J. U. Jung, E. H. Sklan, and B. R. G. Williams. 2019. A CRISPR activation screen identifies genes that protect against Zika virus infection. J. Virol 93:e00211–e00219.

Forde, N., G. B. Duffy, P. A. McGettigan, J. A. Browne, J. P. Mehta, A. K. Kelly, N. Mansouri-Attia, O. Sandra, B. J. Loftus, M. A. Crowe, T. Fair, J. F. Roche, P. Lonergan, and A. C. O. Evans. 2012. Evidence for an early endometrial response to pregnancy in cattle: both dependent upon and independent of interferon tau. Physiol. Genomics 44:799–810.

Gao, G., Y. Cui, and H. Cheng. 2023. Association between retinol binding protein-4 and psoriasis vulgaris: a systematic review and meta-analysis. Front. Med 10:1208969.

Greco, T. M., and I. M. Cristea. 2017. Proteomics tracing the footsteps of infectious disease. Mol. Cell. Proteomics 16:S5–S14.

Guo, Z., M. Zhu, X. Li, H. Xu, and Y. Lv. 2024. Primary goose kidney tubular epithelial cells for goose astrovirus genotype 2 infection: establishment and RNA sequencing analysis. Poult. Sci 103:103774.

Huntzinger, E., J. Sinteff, B. Morlet, and B. Séraphin. 2023. HELZ2: a new, interferon-regulated, human 3′-5′ exoribonuclease of the RNB family is expressed from a non-canonical initiation codon. Nucl. Acids Res 51:9279–9293.

Jakubczak, A., M. Kowalczyk, I. Mazurkiewicz, and M. Kondracki. 2021. Detection of mink astrovirus in Poland and further phylogenetic comparison with other European and Canadian astroviruses. Virus Genes 57:258–265.

Kim, T. H., and H. Zhou. 2015. Functional analysis of chicken IRF7 in response to dsRNA analog poly (I:C) by integrating overexpression and knockdown. Plos One 10:e0133450.

Kirschner, K. M., J. F. W. Braun, C. L. Jacobi, L. J. Rudigier, A. B. Persson, and H. Scholz. 2014. Amine oxidase copper-containing 1 (AOC1) is a downstream target gene of the Wilms tumor protein, WT1, during kidney development. J. Biol. Chem 289:24452–24462.

Kristiansen, H., H. H. Gad, S. Eskildsen-Larsen, P. Despres, and R. Hartmann. 2011. The oligoadenylate synthetase family: An ancient protein family with multiple antiviral activities. J. Interferon. Cytokine Res 31:41–47.

Li, P., G. Lu, L. Wang, Y. Cui, Z. Wu, S. Chen, J. Li, X. Wen, H. Zhang, S. Mu, F. Zhang, and Y. Li. 2016. A rare nonsynonymous variant in the lipid metabolic gene HELZ2 related to primary biliary cirrhosis in Chinese Han. Allerg. Asthma Clin. Immunol 12:14.

Li, C., C. Gao, Q. Fu, B. Su, and J. Chen. 2017. Identification and expression analysis of fetuin B (FETUB) in turbot (Scophthalmus maximus L.) mucosal barriers following bacterial challenge. Fish Shellfish Immunol 68:386–394.

Li, J. J., Y. Yin, H. L. Yang, C. W. Yang, C. L. Yu, Y. Wang, H. D. Yin, T. Lian, H. Peng, Q. Zhu, and Y. P. Liu. 2020. mRNA expression and functional analysis of chicken IFIT5 after infected with Newcastle disease virus. Infect. Genet. Evol 86:104585.

Li, J. Y., W. Q. Hu, T. N. Liu, H. H. Zhang, T. Opriessnig, and C. T. Xiao. 2021. Isolation and evolutionary analyses of gout-associated goose astrovirus causing disease in experimentally infected chickens. Poult. Sci 100:543–552.

Li, H., Z. Kang, C. Wan, F. Zhang, M. Tan, Y. Zeng, C. Wu, Y. Huang, Q. Su, and X. Guo. 2023. Rapid diagnosis of different goose astrovirus genotypes with Taqman-based duplex real-time quantitative PCR. Poult. Sci 102:102730.

Liu, C., L. Li, J. Dong, J. Zhang, Y. Huang, Q. Zhai, Y. Xiang, J. Jin, X. Huang, G. Wang, M. Sun, and M. Liao. 2023. Global analysis of gene expression profiles and gout symptoms in goslings infected with goose astrovirus. Vet. Microbiol 279:109677.

Lu, R., X. Wang, W. Zhao, P. Wang, S. Zhao, X. Zhao, and D. Wang. 2022. Comparative transcriptome and proteome profiles reveal the regulation mechanism of low temperature on garlic greening. Food Res. Int 161:111823.

Madeley, C. R., and V. P. Cosgrove. 1975. Viruses in infantile gastroenteritis. Lancet 306:124.

Marques, J., J. Anwar, S. Eskildsen-Larsen, D. Rebouillat, S. R. Paludan, G. Sen, B. R. G. Williams, and R. Hartmann. 2008. The p59 oligoadenylate synthetase-like protein possesses antiviral activity that requires the C-terminal ubiquitin-like domain. J. Gen. Virol 89:2767–2772.

Miao, X., J. Ma, X. Miu, H. Zhang, Y. Geng, W. Hu, Y. Deng, and N. Li. 2023. Integrated transcriptome and proteome analysis the molecular mechanisms of nutritional quality in 'Chenggu-32' and 'Koroneiki' olives fruits (Olea europaea L.). J. Plant Physiol 288:154072.

Montenegro, D., J. Zhao, H. J. Kim, I. O. Shmarakov, W. S. Blaner, and J. R. Sparrow. 2022. Products of the visual cycle are detected in mice lacking retinol binding protein 4, the only known vitamin A carrier in plasma. J. Biol. Chem 298:102722.

Neves, E. S., I. H. Mendenhall, S. A. Borthwick, Y. C. F. Su, and G. J. D. Smith. 2021. Genetic diversity and expanded host range of astroviruses detected in small mammals in Singapore. One Health 12:100218.

Opriessnig, T., C. T. Xiao, and P. G. Halbur. 2020. Porcine astrovirus Type 5-associated enteritis in pigs. J. Comp Pathol 181:38–46.

Perduca, M., S. Nicolis, B. Mannucci, M. Galliano, and H. L. Monaco. 2018. Human plasma retinol-binding protein (RBP4) is also a fatty acid-binding protein. Biochimica. et Biophysica. Acta (BBA) - Mol. Cell Biol. Lip. 1863:458–466.

Richardson, R. B., M. B. Ohlson, J. L. Eitson, A. Kumar, M. B. McDougal, I. N. Boys, K. B. Mar, P. C. De La Cruz-Rivera, C. Douglas, G. Konopka, C. Xing, and J. W. Schoggins. 2018. A CRISPR screen identifies IFI6 as an ER-resident interferon effector that blocks flavivirus replication. Nat. Microbiol 3:1214–1223.

Ritchie, M. D., E. R. Holzinger, R. Li, S. A. Pendergrass, and D. Kim. 2015. Methods of integrating data to uncover genotype-phenotype interactions. Nat. Rev. Genet 16:85–97.

Roach, S. N., and R. A. Langlois. 2021. Intra- and cross-species transmission of astroviruses. Viruses 13:1127.

Rong, E., J. Hu, C. Yang, H. Chen, Z. Wang, X. Liu, W. Liu, C. Lu, P. He, X. Wang, X. Chen, J. Liu, N. Li, and Y. Huang. 2018. Broad-spectrum antiviral functions of duck interferon-induced protein with tetratricopeptide repeats (AvIFIT). Dev. Comp. Immunol 84:71–81.

Sajewicz-Krukowska, J., J. P. Jastrzębski, M. Grzybek, K. Domańska-Blicharz, K. Tarasiuk, and B. Marzec-Kotarska. 2021. Transcriptome sequencing of the spleen reveals antiviral response genes in chickens infected with CAstV. Viruses 13:2374.

Santhakumar, D., M. A. M. S. Rohaim, H. A. Hussein, P. Hawes, H. L. Ferreira, S. Behboudi, M. Iqbal, V. Nair, C. W. Arns, and M. Munir. 2018. Chicken interferon-induced protein with tetratricopeptide repeats 5 antagonizes replication of RNA viruses. Sci. Rep 8:6794.

Schoggins, J. W., S. J. Wilson, M. Panis, M. Y. Murphy, C. T. Jones, P. Bieniasz, and C. M. Rice. 2011. A diverse range of gene products are effectors of the type I interferon antiviral response. Nature 472:481–485.

Shi, J., Q. Jin, X. Zhang, J. Zhao, N. Li, B. Dong, J. Yu, and L. Yao. 2024. The development of a sensitive droplet digital polymerase chain reaction test for quantitative detection of goose astrovirus. Viruses 16:765.

Wan, F., Y. Zhu, F. Wu, X. Huang, Y. Chen, Y. Zhou, H. Li, L. Liang, L. Qin, Q. Wang, and M. He. 2024. Retinol-binding protein 4 as a promising serum biomarker for the diagnosis and prognosis of hepatocellular Carcinoma. Transl. Oncol 45:101979.

Wang, J., X. Gao, Z. Ma, J. Chen, and Y. Liu. 2019a. Analysis of the molecular basis of fruit cracking susceptibility in Litchi chinensis cv. Baitangying by transcriptome and quantitative proteome profiling. J. Plant Physiol. 234-235:106–116.

Wang, Y., S. Yuan, X. Jia, Y. Ge, T. Ling, M. Nie, X. Lan, S. Chen, and A. Xu. 2019b. Mitochondria-localised ZNFX1 functions as a dsRNA sensor to initiate antiviral responses through MAVS. Nat. Cell. Biol 21:1346–1356.

Wang, A. P., S. Zhang, J. Xie, L. L. Gu, S. Wu, Z. Wu, L. Liu, Q. Feng, H. Y. Dong, and S. Y. Zhu. 2021a. Isolation and characterization of a goose astrovirus 1 strain causing fatal gout in goslings, China. Poult Sci. 100:101432.

Wang, J., C. Xu, M. Zeng, H. Yue, and C. Tang. 2021b. Identification of a novel astrovirus in goats in China. Infect. Genet. Evol 96:105105.

Wu, X., K. Liu, R. Jia, Y. Pan, M. Wang, S. Chen, M. Liu, D. Zhu, X. Zhao, Y. Wu, Q. Yang, S. Zhang, J. Huang, L. Zhang, Y. Liu, B. Tian, L. Pan, Y. Yu, M. Ur Rehman, Z. Yin, B. Jing, and A. Cheng. 2020. Duck IFIT5 differentially regulates Tembusu virus replication and inhibits virus-triggered innate immune response. Cytokine 133:155161.

Wu, M. X., Y. Zou, Y. H. Yu, B. X. Chen, Q. W. Zheng, Z. W. Ye, T. Wei, S. Q. Ye, L. Q. Guo, and J. F. Lin. 2021. Comparative transcriptome and proteome provide new insights into the regulatory mechanisms of the postharvest deterioration of Pleurotus tuoliensis fruitbodies during storage. Food Res. Int 147:110540.

Xing, J., L. Xie, X. Qi, G. Liu, M. F. Akhtar, X. Li, G. Bou, D. Bai, Y. Zhao, M. Dugarjaviin, and X. Zhang. 2023. Integrated analysis of transcriptome and proteome for exploring mechanism of promoting proliferation of equine satellite cells associated with leucine. Comp. Biochem. Physiol. Part D Genom. Proteomics 48:101118.

Xu, L., Z. Wu, Y. He, B. Jiang, Y. Cheng, M. Wang, R. Jia, D. Zhu, M. Liu, X. Zhao, Q. Yang, Y. Wu, S. Zhang, J. Huang, X. Ou, D. Sun, A. Cheng, and S. Chen. 2024. Molecular characterization of a virulent goose astrovirus genotype-2 with high mortality in vitro and in vivo. Poult. Sci 103:103585.

Yang, T., F. Zhang, L. Zhai, W. He, Z. Tan, Y. Sun, Y. Wang, L. Liu, C. Ning, W. Zhou, H. Ao, C. Wang, and Y. Yu. 2018. Transcriptome of porcine PBMCs over two generations reveals key genes and pathways associated with variable antibody responses post PRRSV vaccination. Sci. Rep 8:2460.

Zhang, B., X. Liu, W. Chen, and L. Chen. 2013. IFIT5 potentiates anti-viral response through enhancing innate immune signaling pathways. Acta Biochim Biophys Sin (Shanghai) 45:867–874.

Zhang, Y., F. Wang, N. Liu, L. Yang, and D. Zhang. 2017. Complete genome sequence of a novel avastrovirus in goose. Arch. Virol 162:2135–2139.

Zhang, X., W. Zhang, Y. Liu, H. Qi, C. Hao, W. Zhang, M. Gao, J. Wang, and B. Ma. 2019. Molecular cloning and mRNA expression of IFIT5 in tissues of ducklings infected with virulent duck hepatitis A virus type 3. Res. Vet. Sci 124:256–262.

Zhang, F., H. Li, Q. Wei, Q. Xie, Y. Zeng, C. Wu, Q. Yang, J. Tan, M. Tan, and Z. Kang. 2022. Isolation and phylogenetic analysis of goose astrovirus type 1 from goslings with gout in Jiangxi province, China. Poult Sci. 101:101800.

Zhu, J., A. Ghosh, and S. N. Sarkar. 2015. OASL—a new player in controlling antiviral innate immunity. Curr. Opin. Virol 12:15–19.